

Improvement of geometry and size of a neutron production target for a higher intensity electron accelerator-driven pulsed neutron source

Takuma Tashiro¹, Hirotaka Sato^{1*}, and Takashi Kamiyama¹

¹Graduate School of Engineering, Hokkaido University, Kita-13 Nishi-8, Kita-ku, Sapporo, Hokkaido 060-8628, Japan

Abstract. At the pulsed neutron source facility based on an electron linear accelerator at Hokkaido University, HUNS (Hokkaido University Neutron Source), high wavelength-resolution time-of-flight (TOF) neutron imaging experiments are performed using a decoupled thermal neutron moderator system. However, the neutron intensity is lower than that of a coupled moderator system due to the narrow neutron pulse. To increase the neutron intensity, we considered increasing the neutron intensity provided from a neutron production target located at the most upstream of a neutron beamline. In this study, we improved the target geometry and size to realize a neutron source with not only narrower pulse but also higher intensity. By using particle transport simulation calculations, the target-moderator-in-line geometry was proposed, thereby enhancing the coupling between target and moderator in the in-line geometry. Additionally, enlarging the target size resulted in a reduction of photons entering the neutron beamline owing to the self-shielding effect of the target. In the performance evaluation experiment, the neutron intensity successfully increased by a factor of 2.25, and the spread of the neutron pulse width was suppressed, nevertheless a significant increase in the photon flux.

1 Introduction

The number of merits exist in using a compact neutron source. The relatively compact facility offers the advantage of enabling challenging neutron beam applications with a high degree of on-demand flexibility. The Hokkaido University Neutron Source (HUNS) is an electron linear accelerator-driven pulsed neutron facility, which has achieved significant milestones in both academic and industrial fields [1]. HUNS offers three types of neutron sources: cold, thermal, and fast neutron sources, providing neutron beams with a wide energy range from meV to MeV.

In particular, the decoupled-type neutron source beamline at HUNS has been utilized for high wavelength-resolution neutron Bragg edge imaging experiments with its short-pulsed neutrons and the TOF method [2]. In this beamline, the pulse width of meV-order neutrons

* Corresponding author: h.sato@eng.hokudai.ac.jp

has been successfully shortened to several tens of microseconds by inserting cadmium decoupler, which strongly absorbs neutrons below 0.5 eV, between the moderator and the reflector in the neutron source. In addition, the neutron transport efficiency has been enhanced by installing a supermirror guide-tube to compensate for the neutron intensity reduction caused by the decoupler. Obviously, the neutron intensity of the decoupled-type neutron source is still lower than that of the coupled-type neutron source without the cadmium decoupler. To achieve high-precision Bragg edge imaging within a shorter time, it is essential to enhance the neutron intensity of the decoupled-type neutron source beamline.

In this study, we explored enhancing neutron intensity by improving a neutron production target system located at the most upstream of a neutron beamline. In the past, intensity improvements at HUNS have continued by optimizations of the neutron moderator, the neutron reflector, and the supermirror guide-tube. As a new approach, we considered improving the target system at the most upstream, which can increase the whole neutron intensity. The objective of this study was to improve the geometry and size of a neutron production target for a higher intensity electron accelerator-driven pulsed neutron source.

2 Target system study by particle transport calculations

The target system was studied through simulation calculations using the particle transport Monte-Carlo code PHITS ver.3.27 [3]. The evaluated nuclear data we used was JENDL-4.0. We optimized the geometry and size of the target as a target system improvement. Traditionally, neutron beamlines at HUNS are set in the “wing” geometry. In this study, for improvement from this traditional geometry, we considered two geometries in order: the flux-trap target geometry at first, and the target-moderator-in-line geometry (“slab” geometry) as an advanced form. Fig. 1 shows a geometry of the current status of a neutron beamline using a decoupled thermal moderator at HUNS. To evaluate the improved target system, we compared the neutron flux, photon flux, and neutron pulse width of the improved system with those of the current system.

As a first step, we focused on the flux-trap target geometry as shown in Fig. 2. Lead slabs were used as a front and a rear neutron production targets in calculation. The electron beam was a cylindrical beam with an energy of 32 MeV and a diameter of 10 mm. We checked its neutron and photon production states with changing the front-stage target thickness, t . The neutron flux exhibited its highest intensity at $t = 15$ mm, but we observed that photons, electrons, and positrons contributing to photo-nuclear neutron production are diverged by the front-stage target. High energy photons emitted from the primary electron beam are emitted

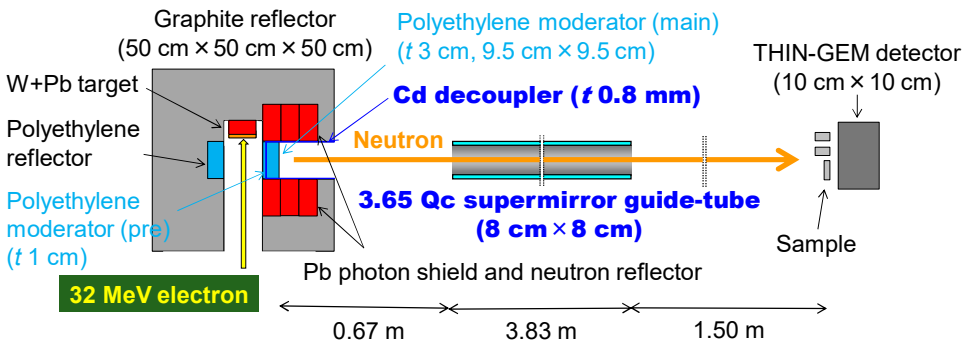


Fig. 1. Geometry of the current status of a neutron beamline using a decoupled thermal moderator at HUNS.

from the front-stage target. Next, these photons cause electron-positron pair productions. These secondary electrons and positrons emit lower energy photons owing to bremsstrahlung and pair annihilation. These lower energy photons contribute photo-nuclear neutron production again. However, each particle did not reach the rear-stage target sufficiently, indicating an inability to produce neutrons by the rear-stage target.

Next, we considered the target-moderator-in-line geometry which has a straight alignment of the neutron target, moderator, and neutron beamline. In general, this target geometry has been considered to increase neutron intensity, but has been avoided because it would increase the number of fast neutrons and photons mixed into the neutron beam. However, we considered increasing the size of the target to increase the target's self-shielding effect against photons, thereby reducing the number of photons mixed into the neutron beamline. Of course, neutrons could also be shielded, but we supposed that the shielding effect for MeV neutrons, 5 barns, would be smaller than that for several-ten MeV photons, 23 barns. This is because neutrons are more difficult to shield with lead than photons. In addition, producing photoneutrons would increase owing to the larger volume of the lead target that generates neutrons. In the target-moderator-in-line geometry, the main point of neutron production, the point of incidence of the electron beam, is not far from the moderator position. This has an advantage of using a large-volume target that is less effective in the flux-trap geometry. That was expected to be useful for the GEM-type neutron TOF-imaging detector with ^{10}B converter using at HUNS [4] to separate fast neutrons by the TOF method and photons by the signal/noise discrimination function.

The calculation geometry is shown in Fig. 3. The schematics of the main target and the sub-target are shown in Fig. 4 and Fig. 5, respectively. The entire target consists of the main target and the sub-target. The main target is a conventional target used in HUNS. The overall target size was increased with lead sub-target by surrounding around the main target. In this

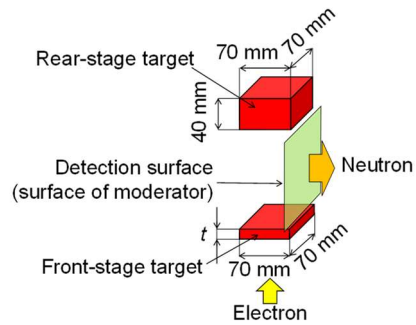


Fig. 2. Calculation geometry of the flux-trap target geometry.

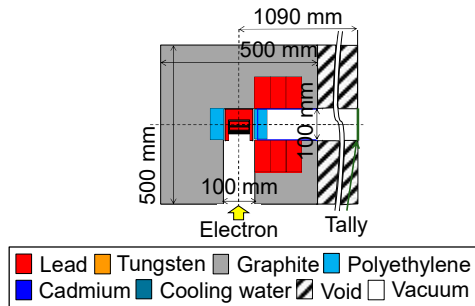


Fig. 3. Calculation geometry of the target-moderator-in-line geometry.

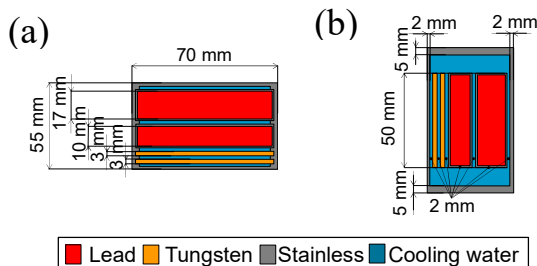


Fig. 4. Schematic of the main target. (a) Top view cross-section. (b) Side view cross-section.

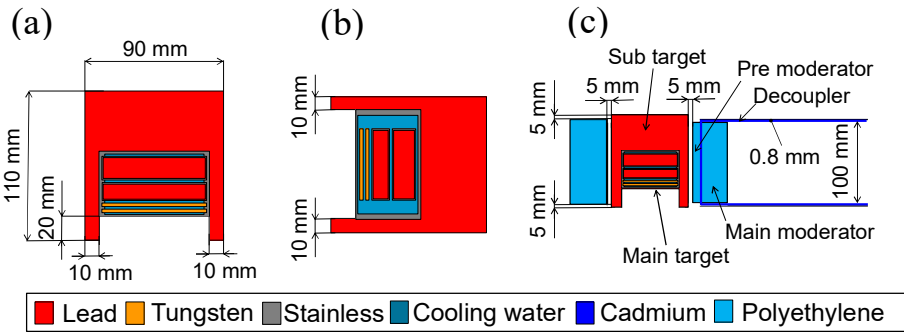


Fig. 5. Schematic of the overall target. (a) Top view cross-section. (b) Side view cross-section. (c) Top view cross-section with moderator and decoupler.

geometry, neutron flux, photon flux, and 4-6 meV neutron pulse shape were calculated at a distance of 1 m from the moderator surface. The surface detector was used in the calculation.

Calculated results of the neutron energy spectrum, photon energy spectrum, and neutron pulse shape are shown in Figs. 6, 7, and 8. Note that the vertical axis depends on the bin width of horizontal axis. In Fig. 6, the range from 10^{-10} MeV to 10^3 MeV is logarithmically equally divided into 150 points. In Fig. 7, the range from 10^{-2} MeV to 35 MeV is logarithmically equally divided into 100 points. As shown in Fig. 6 neutron intensities increase in whole neutron energy. The further increase in fast neutron region is considering to be owing to the increased fraction of direct delivery from the target, as the target is in the direct line of sight from the neutron beamline. The total neutron flux below 0.5 eV is found to be 1.34 times higher than that of the conventional system. The photon energy spectra show the change in shape compared to the conventional system. The reason for the increase in 1-30 MeV photons is considering to be owing to the increased fraction of direct delivery from the target. The decrease in 0.1-1 MeV photons is owing to the self-shielding effect of lead target, as low-energy photons are in an energy band that is easily shielded. Overall, the total amount of photons was the same as the conventional amount. These results for the target-moderator-in-line geometry show that the enlarging the neutron target is effective to increase the neutron flux while suppressing the increasing photons. Fig. 8 shows calculated neutron pulse shapes for 4-6 meV neutrons at the detector position in the conventional system and the improved system. These results are preliminary and insufficient ones because these are very poor in terms of statistics due to our calculation deficiencies. Thus, we evaluated the neutron pulse width using the curve fitting. The red curves represent fitting curves obtained by a Gaussian

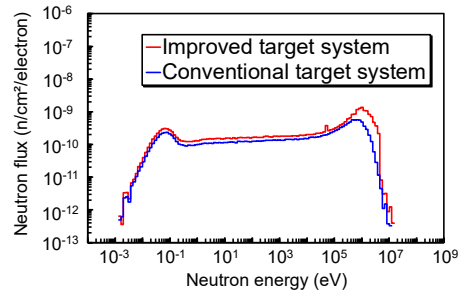


Fig. 6. Neutron energy spectra obtained with the improved target system and the conventional target system.

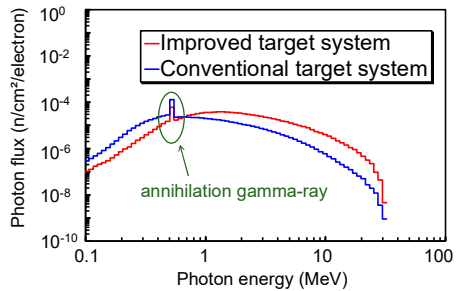


Fig. 7. Photon energy spectra obtained with the improved target system and the conventional target system.

The reason for the increase in 1-30 MeV photons is considering to be owing to the increased fraction of direct delivery from the target. The decrease in 0.1-1 MeV photons is owing to the self-shielding effect of lead target, as low-energy photons are in an energy band that is easily shielded. Overall, the total amount of photons was the same as the conventional amount. These results for the target-moderator-in-line geometry show that the enlarging the neutron target is effective to increase the neutron flux while suppressing the increasing photons. Fig. 8 shows calculated neutron pulse shapes for 4-6 meV neutrons at the detector position in the conventional system and the improved system. These results are preliminary and insufficient ones because these are very poor in terms of statistics due to our calculation deficiencies. Thus, we evaluated the neutron pulse width using the curve fitting. The red curves represent fitting curves obtained by a Gaussian

function for evaluation of neutron pulse widths. As a result, we found that neutron pulse width was unchanged before and after the improvement. Since the neutron pulse width is affected by the thickness of the moderator in the direction of the neutron beam, the neutron pulse width spread was unchanged.

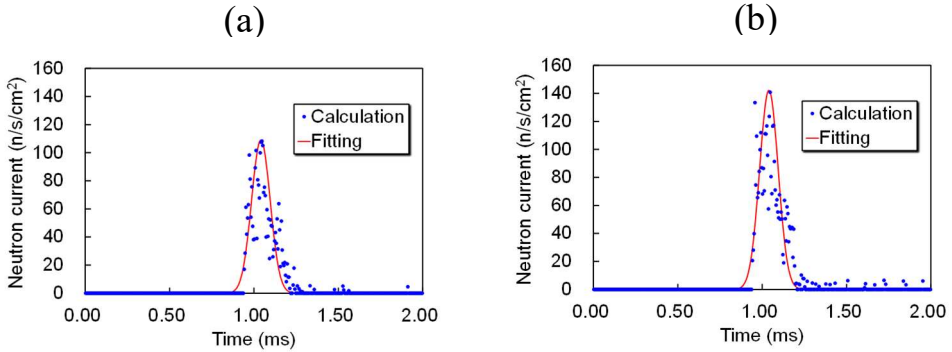


Fig. 8. Neutron pulse shape for 4-6 meV neutrons. (a) Neutron pulse shape obtained with the conventional system. (b) Neutron pulse shape obtained with the improved system.

3 Experimental performance evaluation of the in-line geometry

We carried on performance evaluation experiments of the proposed system at HUNS. Three measurements were conducted for neutron spectrum, photon dose, and neutron pulse profile in the neutron energy range around 5 meV. The repetition frequency of the accelerator was 70 Hz for neutron measurements and 10 Hz for photon measurements. Electron beam power was 2.3 kW and electron beam energy was 32 MeV. Neutron flight path length was 6.05 m.

The GEM-type TOF-imaging detector [4] was used to measure neutron spectrum and neutron pulse profile. Neutron pulse profile was evaluated by measuring the Bragg edge neutron transmission spectrum of α -Fe of 1 cm thickness and comparing the sharpness of the {110} Bragg edges. The results of neutron counting rate spectra and neutron transmission spectra are shown in Figs. 9 and 10. The neutron counting rate spectra show that the neutron spectral shape remains unchanged before and after the improvement and the neutron intensity is increasing. As a result, the neutron flux increased by a factor of 2.25. This value is quite different from that of simulation calculation. Unfortunately, we did not identify this reason. The different point between calculation and experiment is the detector position. However, this is not a conclusive reason. This is a problem that must be resolved in the future work.

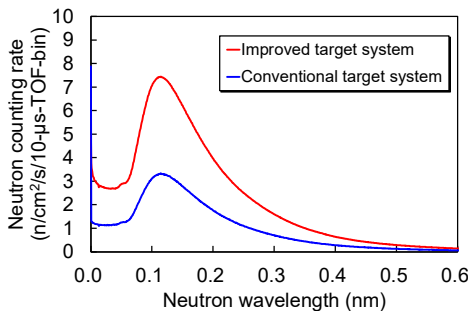


Fig. 9. Neutron wavelength spectra obtained with the improved target system and the conventional target system.

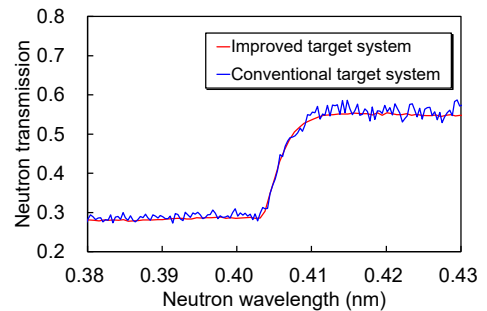


Fig. 10. {110} Bragg edge spectra of α -Fe obtained with the improved target system and the conventional target system.

On the other hand, the neutron transmission spectra show no change in the sharpness of the Bragg edge, namely, the pulse width obtained in the improved system was found to be comparable to those of conventional high wavelength-resolution system.

For measuring the photon doses an ionization chamber dosimeter was used. Due to the sensitivity of the ionization chamber to both thermal and epithermal neutrons [5], boron rubber with 80% boron concentration and 20 mm thickness were put in front of the detector to shield against these neutrons. The photon dose obtained with the improved system was 82.7 mSv/h, a significant increase compared to the 3.89 mSv/h obtained with the conventional system. One possible reason for this large increase is that the detector is now positioned farther away from the target than initially calculated in the simulation, making it more susceptible to photons from the target due to the target-moderator-in-line geometry. It is also possible that the neutron flux increased across all energy bands, and that the photon dose values might have been induced by fast neutrons that were not shielded by boron. On the other hand, when compared to the photon dose directly reached from the fast neutron source at HUNS, the photon dose was found to be approximately one-third of that from the fast neutron source at HUNS. The fast neutron source at HUNS is configured in in-line geometry, but the target size is small, 7 cm × 7 cm × 7 cm. From this, the self-shielding effect of neutrons is at work owing to the enlargement of the lead target.

4 Conclusion

As a result of the investigation of target system using particle transport simulation, we devised target-moderator-in-line geometry. As a result of conducting performance evaluation experiments on the optimized TMRA, the neutron flux was increased by a factor of 2.25, while maintaining an equivalent neutron pulse width to that of the conventional system. On the other hand, the results for photon flux showed increase compared to the conventional system. Having successfully increased neutron intensity while suppressing the spread of neutron pulse width, the upcoming research will focus on the shielding of the increased photon emissions.

After all, the in-line geometry is the same as the “slab” geometry [6]. In addition, in this type of geometry, increase of fast neutrons affects on the S/N ratio of neutron scattering experiments and the radiation shielding. However, it is a new point of the present study that an effective system for neutron Bragg-edge transmission imaging instrument at HUNS is found.

The authors are thankful to Mr. Hiroki Nagakura and Mr. Koh-ichi Sato of Hokkaido University for accelerator operations and experimental assistances. This work was supported by JSPS KAKENHI Grant Number JP22H01998.

References

1. M. Furusaka, H. Sato, T. Kamiyama, M. Ohnuma, Y. Kiyonagi, *Physics Procedia* **60**, 167 (2014)
2. H. Sato, T. Sasaki, T. Moriya, H. Ishikawa, T. Kamiyama, M. Furusaka, *Physica B: Condensed Matter* **551**, 452 (2018)
3. T. Sato, Y. Iwamoto, S. Hashimoto, T. Ogawa, T. Furuta, S. Abe, T. Kai, P. Tsai, N. Matsuda, H. Iwase, H. Shigyo, L. Sihver, K. Niita, *Journal of Nuclear Science and Technology* **55**, 684 (2018)

4. S. Uno, T. Uchida, M. Sekimoto, T. Murakami, K. Miyama, M. Shoji, E. Nakano, T. Koike, K. Moriya, H. Satoh, T. Kamiyama, Y. Kiyonagi, *Physics Procedia* **26**, 142 (2012)
5. Y. Uwamino, H. Mukai, *Radioisotopes* **71**, 41 (2022) (in Japanese)
6. Y. Kiyonagi, *Journal of Nuclear Science and Technology* **22**, 934 (1985)